An investigation of first-order transition across charge ordered and ferromagnetic phases in $Gd_{0.5}Sr_{0.5}MnO_3$ single crystals by magnetic and magnetotransport studies

2010 J. Phys.: Condens. Matter 22 026005

(http://iopscience.iop.org/0953-8984/22/2/026005)

J. Phys.: Condens. Matter **22** (2010) 026005 (7pp) doi:10.1088/0953-8984/22/2/026005

An investigation of first-order transition across charge ordered and ferromagnetic phases in $Gd_{0.5}Sr_{0.5}MnO_3$ single crystals by magnetic and magnetotransport studies

Aditya A Wagh[1], P S Anil Kumar[1], H L Bhat[1,2] and Suja Elizabeth[1]

[1] Department of Physics, Indian Institute of Science, C V Raman Avenue, Bangalore 560012, India
[2] Centre for Liquid Crystal Research, Jalahalli, Bangalore 560013, India

E-mail: waghaditya@physics.iisc.ernet.in

Received 28 August 2009, in final form 1 November 2009
Published 10 December 2009
Online at stacks.iop.org/JPhysCM/22/026005

Abstract

Gadolinium strontium manganite single crystals of the composition $Gd_{0.5}Sr_{0.5}MnO_3$ were grown using the optical float zone method. We report here the magnetic and magnetotransport properties of these crystals. A large magnetoresistance $\sim 10^9$% was observed at 45 K under the application of a 110 kOe field. We have observed notable thermomagnetic anomalies such as open hysteresis loops across the broadened first-order transition between the charge order insulator and the ferromagnetic metallic phase while traversing the magnetic field–temperature (H–T) plane isothermally or isomagnetically. In order to discern the cause of these observed anomalies, the H–T phase diagram for $Gd_{0.5}Sr_{0.5}MnO_3$ is formulated using the magnetization–field (M–H), magnetization–temperature (M–T) and resistance–temperature (R–T) measurements. The temperature dependence of the critical field (i.e. H_{up}, the field required for transformation to the ferromagnetic metallic phase) is non-monotonic. We note that the non-monotonic variation of the supercooling limit is anomalous according to the classical concepts of the first-order phase transition. Accordingly, H_{up} values below $\sim$20 K are unsuitable to represent the supercooling limit. It is possible that the nature of the metastable states responsible for the observed open hysteresis loops is different from that of the supercooled ones.

(Some figures in this article are in colour only in the electronic version)

1. Introduction

Mixed valence perovskites $A_{1-x}A'_xMnO_3$ with rare earth ions (A = La, Pr, Nd, ...) doped with divalent ions (A′ = Sr and Ca) are known to exhibit interesting properties such as charge ordering (CO), colossal magnetoresistance (CMR), etc [1]. The bicritical features, emerging around the first-order phase transition (FOPT) boundary between the ferromagnetic metallic (FMM) and the charge ordered/orbital ordered (CO/OO) state due to the phase competition, are essential components in CMR physics [2]. There are numerous reports [3–7] on the magnetic and transport properties of the mixed valence manganites which have illustrated the influence of the hole doping (x), the mean size of the radius in the A-site ($\langle r_A \rangle$) and the random disorder, which is the size mismatch at the A-site (i.e. σ^2, variance), on these properties. An investigation on highly mismatched manganites with high values of $\langle r_A \rangle$ has shown that the variance (σ^2) is the most favoured factor for the occurrence of the spin glass insulator state [5]. It is also true that quenched disorder is inevitable in the mixed valence manganites unless these materials are synthesized by special methods [6]. A report, based on the investigations of A-site ordered and disordered perovskites, has claimed that the random potential in a disordered system is not only responsible for the spin glass state but also has a key role in the CMR phenomenon [6].

There are several investigations on CMR materials possessing quenched disorder or weak disorder [8–18]. Kuwahara *et al* [8] and Tokura *et al* [9] reported anomalous thermomagnetic history effects in $Nd_{0.5}Sr_{0.5}MnO_3$ (NSMO) single crystal. Manekar *et al* [10] observed anomalous open hysteresis loops in a non-perovskite system such as Al-doped $CeFe_2$. They put forward the concept of an interplay between kinetic arrest and supercooling to explain the observed anomalies and further suggested that this concept would explain the anomalies found in NSMO, which was later verified by Rawat *et al* [11]. The observed anomalous thermomagnetic history effects have been explained with the help of kinetically arrested metastable states in diverse materials [10–14]. Apart from the development of the kinetic arrest model, Sharma *et al* [18] have recently proposed that the freezing of structural interface motion forms the origin for glassiness in $La_{0.215}Pr_{0.41}Ca_{3/8}MnO_3$. There have been some very interesting studies done recently on the phase separated manganites in order to observe phase fluctuations near the transition. In addition, time resolved transformations between the charge ordered insulating phase and the ferromagnetic metallic phase have also been observed in mesoscopic manganite structures [19, 20].

After the investigations on magneto-electric materials in the 70s [21], the past decade has seen a resurgence of interest in the study of multiferroics [22–27]. The materials investigated so far show diverse origins for ferroelectricity. Large magneto-electric effects were discovered in the rare earth manganites $AMnO_3$ (A = Gd, Tb, Dy, ...) [27], but there are relatively few investigations of this behaviour in doped manganese oxides [28].

$Gd_{0.5}Sr_{0.5}MnO_3$ (GSMO) is one such compound which has been reported to show the development of spontaneous electric polarization in the presence of magnetic fields [28]. Garcia *et al* [29] explored the nature of the CMR in polycrystalline GSMO and assigned irreversibility and anomalies in the magnetization, magnetoresistance and magnetostriction isotherms below 90 K to the onset of the charge ordering below this temperature. Their linear thermal expansion data supported this assumption. Neutron diffraction studies on GSMO revealed that there is no long range magnetic ordering at low temperatures [29]. In addition, the coexistence of charge ordered insulator (COI) and cluster glass (CG) states has been claimed [29] to occur below 42 K. The electric polarization studies of a GSMO single crystal showed that the phase transition from CG + COI to FMM (under 100 kOe at 4.5 K) occurs with a change in the electric polarization ($\Delta P \sim 100\ \mu C\ m^{-2}$) [28].

In the case of GSMO, $\langle r_A \rangle$ is 1.33 Å (the effective ionic radii r_A used are from [30] and the coordination number considered for Gd^{3+} and Sr^{2+} is 12) and σ^2 is 0.0133 $Å^2$. The presence of glassy dynamics at low temperatures in this highly disordered CMR material motivated us to study the FOPT between the FMM and COI phases in this system. In this paper, we report electric, magnetic and magnetotransport studies on GSMO single crystals. We report anomalies such as the open hysteresis loop observed across a broadened FOPT while scanning the H–T plane isothermally or isomagnetically. We have formulated the H–T phase diagram for GSMO and discuss here a few interesting features in it such as the non-monotonic variation of the supercooling limit, which is an anomalous behaviour according to the classical ideas of FOPT.

2. Experimental details

Polycrystalline $Gd_{0.5}Sr_{0.5}MnO_3$ was prepared by the solid state reaction, where Gd_2O_3, Sr_2CO_3 and MnO_2 precursors were homogenized and sintered at 1200 °C in air for 36 h with intermediate grinding. The single phase nature was confirmed by x-ray powder diffraction (XRD) (Bruker D8 advance x-ray diffractometer). The synthesized powder was pressed into rods under 70 MPa pressure using a hydrostatic press. Subsequently, these rods were sintered at 1400 °C in air for 24 h. Crystals were grown by the float zone method using a four mirror optical image furnace (FZ-T-10000-H-VI-VP procured from Crystal Systems Inc, Japan). The feed rod and seed rod rotation rates were maintained at 45 and 25 rpm, respectively. The air flow rate was 5 l min^{-1} and the growth rate was 1 mm h^{-1}. The crystal grown was ~6 mm in diameter and ~27 mm long. Each experimental sample was checked for single crystallinity by taking a Laue photograph. The powder XRD data were then obtained for the crushed crystal and the Rietveld refinement was performed.

The electric transport measurements were carried out using a four probe or two probe method appropriately according to the sample resistance. The typical dimensions of the samples used for measurements were 3 mm × 3 mm × 0.5 mm. In order to measure the high resistance of the sample at very low temperatures, gold pads were thermally evaporated on the surface with a spacing ~70 μm. The typical dimensions of the gold pads were 1 mm × 1 mm with a thickness of ~50 nm. The contacts were made using silver paste. A Keithley Sourcemeter unit 2612 (SU) was used to measure very high resistance values (~10^{10} Ω).

The magnetotransport measurements were performed, with the applied magnetic field (maximum field up to 110 kOe) perpendicular to the direction of the electric current, in the temperature range 4.2–300 K inside a Janis Magneto Cryostat. Helium exchange gas was used as a coolant. The DC magnetization was studied using a commercial 14 T vibrating sample magnetometer (Quantum Design, PPMS-VSM) in the temperature range 3–300 K. In both measurements, the magnetic field was applied along the direction of growth of the single crystal.

3. Results and discussion

3.1. Crystal structure

The GSMO is reported to be orthorhombic with the space group *Pbnm* [29, 31] or (in different setting) *Pnma* [32]. In the present study, the crystal structure of the GSMO was refined in the orthorhombic space group *Pbnm*. Figure 1 shows the XRD pattern (I_{obs}) obtained from the crushed crystal, the Rietveld fit (I_{cal}) and the difference pattern ($I_{obs} - I_{cal}$). The unit cell parameters obtained from the refinement are: $a = 5.4275(4)$ Å, $b = 5.4225(3)$ Å and $c = 7.6379(2)$ Å, which satisfies the condition $(c/\sqrt{2}) < b < a$. This

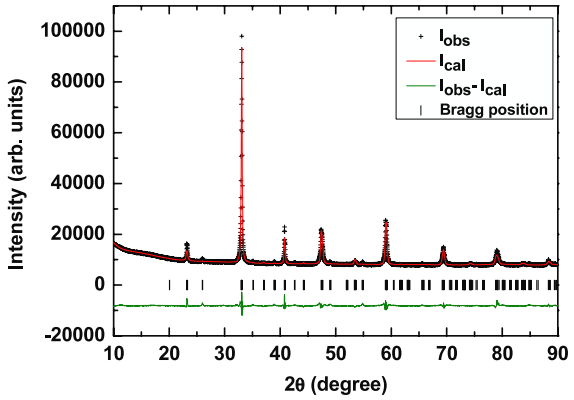

Figure 1. X-ray powder diffraction pattern of a crushed single crystal of GSMO at room temperature. The fit of Rietveld refinement, the difference pattern and the Bragg peak positions are shown. Goodness-of-fit parameters for the structural refinement are: $R_p = 1.64\%$, $R_{wp} = 2.58\%$ and $\chi^2 = 6.399$.

is different from the conditions required for both O and O′ distortions. Woodward *et al* [32] also observed this in the $Ln_{0.5}Sr_{0.5}MnO_3$ series (Ln = La, Pr, Nd, Sm, Gd, ...) with a *Pnma* setting.

3.2. Magnetotransport and magnetic studies

Figure 2(a) illustrates the temperature dependence of the resistance under the application of magnetic fields up to 110 kOe. The measurements were carried out by the four probe method. In the absence of the magnetic field, the resistance increases monotonically with a decrease in temperature; this has been explained [29] using the charge localization (CL) associated with lattice distortion. Below 40 K, the resistance attains very high values, beyond the instrument's measurement limit. This semiconducting/insulating behaviour is observed in the entire temperature range and the signature of the charge order (T_{co}), is not reflected in the R–T curve ($T_{co} \sim 90$ K [29], i.e. a crossover from CL to an inhomogeneous CO state). This is in agreement with the previous reports on GSMO [28, 29]. The absence of any signature of CO in the R–T curve near the T_{co} was also reported in $RE_{0.5}Sr_{0.5}MnO_3$ (RE = Dy, Ho, Er) [33]. Under the application of magnetic fields $\geqslant$80 kOe, the insulator–metal (I–M) transition is discernible at low temperatures. This results in a very large magnetoresistance ($MR = 100 \times \{[R(0) - R(H)]/R(H)\}$). Figure 2(b) shows that, at 45 K, under an applied magnetic field of 110 kOe, the magnetoresistance is $\sim 10^9\%$. Below $\sim$70 kOe, no I–M transition is observed throughout the temperature range, thereby giving a relatively small magnitudes of MR; e.g. at 50 K and 70 kOe, MR is $\sim 10^3\%$. The present CMR material indeed poses a challenge in magnetotransport measurements at low temperatures and high magnetic field due to its dynamic and wide range of resistance changes. The detailed discussion and qualitative comparison of the MR properties at low temperatures (down to 5 K) with previous reports are given later.

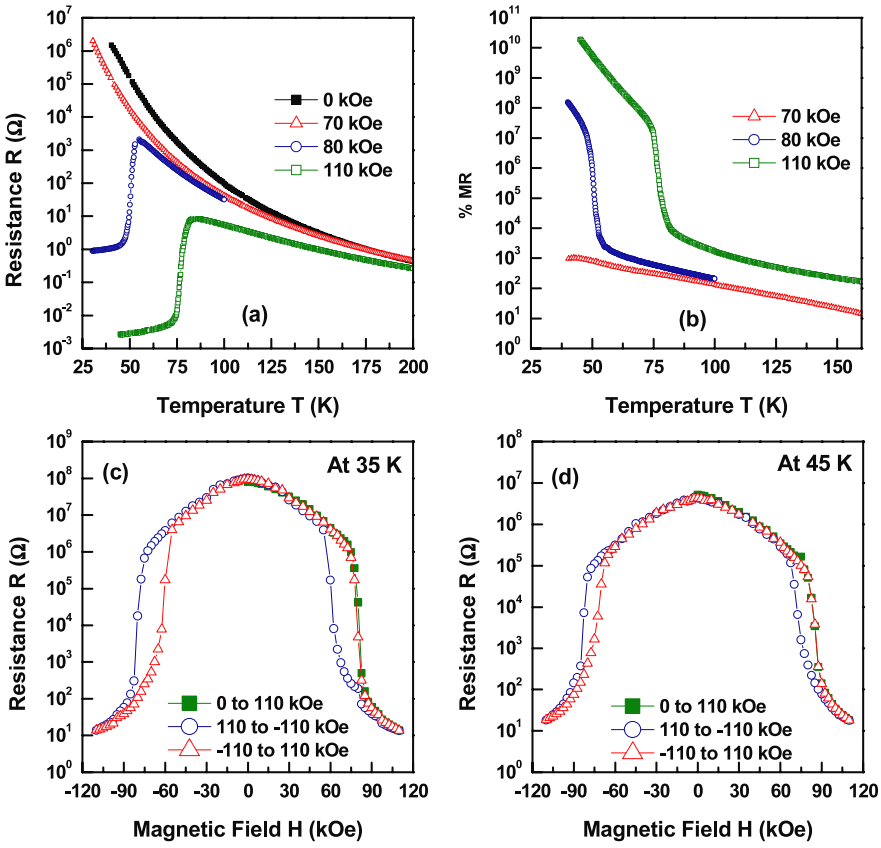

Figure 2. (a) Temperature variation of resistance (ZFC measurement) under application of different magnetic fields. (b) Temperature dependence of magnetoresistance (ZFC measurement) studied under application of different magnetic fields. (c) and (d) Field dependence of resistance studied at two different constant temperatures, 35 and 45 K, respectively.

Figures 2(c) and (d) show the field dependence of resistance studied at two constant temperatures, 35 and 45 K, respectively. These measurements were carried out by the two probe method using an SU. Initially the sample was cooled from room temperature to the desired temperature in a zero magnetic field, and the field was then swept isothermally in a cycle and the resistance was measured. The magnetic field sweeping cycle can be divided into five segments: segment 1: 0–110 kOe, segment 2: 110–0 kOe, segment 3: 0 to −110 kOe, segment 4: −110 to 0 kOe and segment 5: 0–110 kOe (along the initial direction). At 35 K (figure 2(c)), in the first segment, the resistance decreases slowly with the increasing field until the critical upper field, H_{up}, is reached. Around H_{up}, the resistance falls sharply, which is an indication of the I–M transition. Further, in the metallic state, the resistance decreases gradually while the field increases. When the field is reduced in the second segment, the resistivity shows an irreversibility and the M–I transition shifts to a lower field value i.e. H_{dn} ($H_{dn} < H_{up}$). This hysteresis is characteristic of FOPT. It is relevant to note that the virgin R–H curve (in segment 1) is found to merge with the R–H curve in the fifth segment. All the above features are present at 45 K (figure 2(d)), except that the hysteretic region is found to be narrower compared to the loop at 35 K. These observations are in agreement with the previous report [29].

Figure 3(a) shows the temperature dependence of DC magnetization under the application of two different magnetic fields, 500 Oe and 10 kOe. The measurements were carried out with three protocols, namely zero field cooling (ZFC), field cooled cooling (FCC) and field cooled warming (FCW). The temperature ramp rate was ±1.5 K min^{-1} and the measurements were carried out in the range, 5–300 K. Under a magnetic field of 500 Oe, a clear splitting between ZFC and FCW magnetization is seen at 47 K. At an applied field of 10 kOe, the splitting between ZFC and FCW becomes narrower and the splitting point shifts to a lower temperature (∼42 K). This splitting is one of the characteristics of glassy behaviour [29], however mere splitting cannot confirm the occurrence of a spin glass. The shift in the splitting temperature with different fields is a consequence of the balance between the competing magnetic and thermal energy. The plot of inverse susceptibility versus temperature for 500 Oe (figure not shown) reveals that the linear relationship is obeyed only at higher temperatures (greater than 250 K). Small angle neutron scattering studies on GSMO [29] have indicated the presence of short range antiferromagnetic correlations in the CO phase. These correlations could possibly explain the nonlinearity of the inverse susceptibility observed in the relevant temperature range. However, a detailed investigation is required in the extended temperature range (up to 250 K) to understand this feature.

Figure 3(b) shows the temperature dependence of the magnetization under the application of higher magnetic fields. At 50 kOe, a very narrow splitting of the ZFC and FCW magnetization is observed near 37 K. In the case of higher fields, 90 and 120 kOe, a COI to FMM transition is discernible. We have performed the ZFC and FCC magnetization measurements, and a clear thermal hysteresis is observed

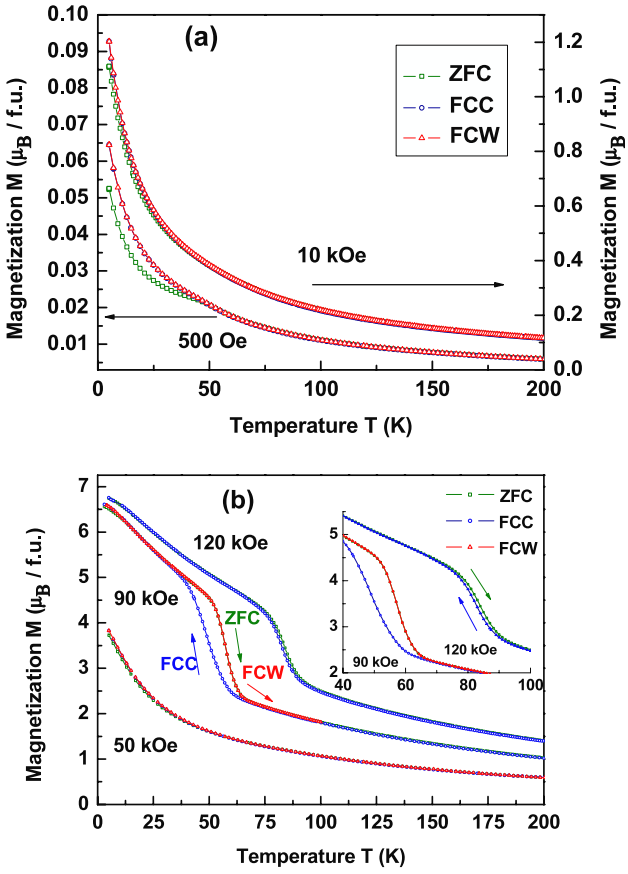

Figure 3. (a) Temperature dependence of magnetization studied under application of different magnetic fields. Splitting between ZFC and FCC/FCW magnetization curves is seen at low magnetic fields, 500 Oe and 10 kOe. (b) Thermal hysteresis corresponding to FOPT at magnetic fields, 90 and 120 kOe. Inset shows magnified thermal hysteresis at 90 and 120 kOe.

across the COI to FMM phase transition which is characteristic of FOPT. The narrow hysteresis, observed at 120 kOe, indicates the suppression of hysteresis with an increase in field strength. At 10 K, and 120 kOe, the observed magnetization is 6.62 μ_B/f.u., which is higher than the 3.5 μ_B/f.u. expected for the Mn^{3+}/Mn^{4+} ratio in GSMO. Hence the magnetic contribution of the rare earth ion (Gd^{3+}) has to be considered. The heavy rare earth ions are known to order only at very low temperatures, and hence a paramagnetic contribution of these ions is expected down to low temperatures. There have been reports on very complex magnetic interactions observed between the Gd^{3+} and Mn^{3+}/Mn^{4+} sublattices in certain Gd-based manganites [34, 35]. Even though the paramagnetic contribution of Gd^{3+} ions could explain the low temperature susceptibility in GSMO, the determination of the exact alignment of spins and the magnetic contribution of the Gd^{3+} ions require further investigations. It may be noted that the magnetization measurement at 90 kOe was initiated by first cooling the sample to 3 K in the absence of a magnetic field.

The magnetization isotherms were studied under applied magnetic fields up to 140 kOe. A similar measurement protocol as in the R–H measurements was used here. The magnetic field was swept at the ramp rate of 80 Oe s^{-1}.

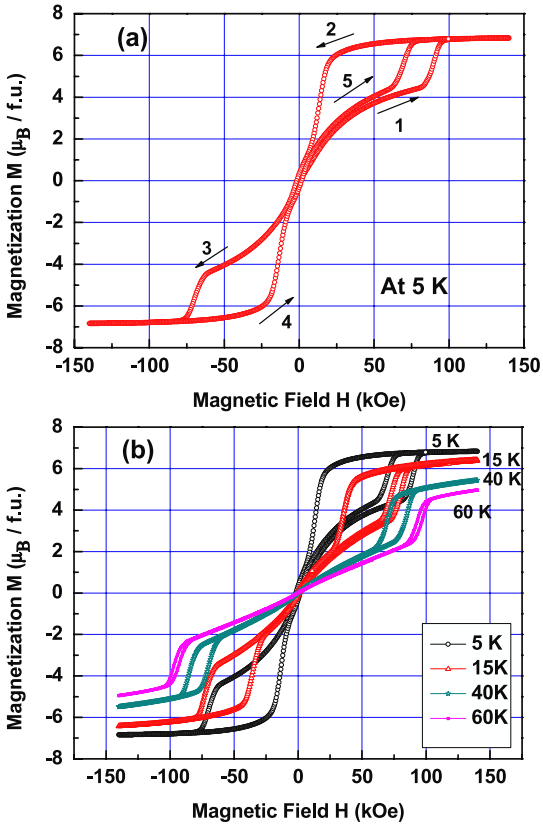

Figure 4. (a) Field dependence of magnetization studied at 5 K. The virgin magnetization curve (segment 1) is observed to lie outside the envelope. (b) Isothermal magnetization curves recorded at different temperatures, 5, 15, 40 and 60 K.

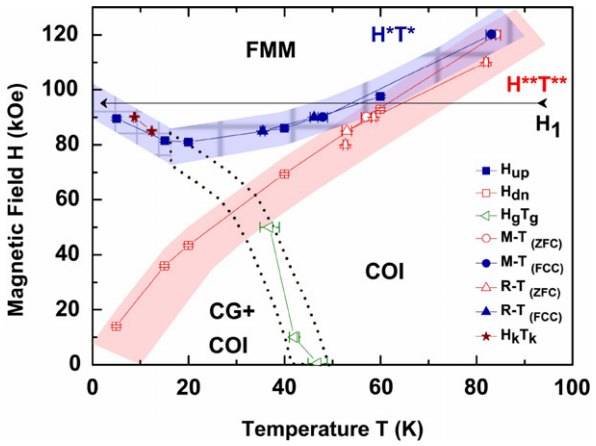

Figure 5. (Colour online) H–T phase diagram for GSMO prepared using M–H, M–T and R–T measurements (the error bar is shown appropriately). Superheating and supercooling limits are shown with the help of the shaded band and the band with a broad grid, respectively. Narrow grid lines are drawn to distinguish the anomolous region corresponding to H_kT_k values (or H_{up} values below ∼20 K) from supercooling limit. The low temperature glassy phase which was claimed to be a CG + COI phase in a previous report [29], is shown in the phase diagram for reference.

Figure 4(a) shows the field dependence of magnetization measured at 5 K. In the first segment (0–140 kOe), close to the critical magnitude of field H_{up}, the magnetization increases sharply. This metamagnetic transition corresponds to a transformation to the FMM phase. The magnetization saturates at higher fields, and at 140 kOe the saturation magnetization is 6.83 μ_B/f.u., which indicates the magnetic contribution of Gd^{3+} ion. This experimental value is close to the calculated value of 7 μ_B/f.u. for GSMO. With a decrease in the magnetic field (segment 2), a reverse phase transition is seen to occur at a lower magnetic field, H_{dn}. Subsequently, it is observed that the M–H curve in the third segment is not symmetric to that in the first segment. Accordingly, the M–H measurement was extended to segment 5. The virgin M–H curve (segment 1) is found to be outside the envelope, a feature not observed in previous studies [28, 29], since the M–H measurements were performed only up to segment 2. This anomaly indicates that the reverse transition from the FMM phase is incomplete at zero magnetic field and a fraction of the FMM phase is present in the material. A remanent magnetization ∼0.33 μ_B/f.u. and a coercive field ∼1370 Oe were observed in the M–H curve at 5 K.

Figure 4(b) illustrates the comparison of the M–H isotherms measured up to 140 kOe at different temperatures (5, 15, 40 and 60 K). The anomalous feature observed at 5 K is also noticeable in the M–H curve at 15 K, but not at 40 K (and 60 K) where the curve in the third/fourth segment is symmetric to that in the first/second segment, indicating that the reverse transition from the FMM phase is complete at zero magnetic field. A broadening of the hysteresis is observed as the temperature is lowered, which is in agreement with previous studies [28, 29].

The FOPT and the observed anomaly are analysed on the basis of the H–T phase diagram formulated using the above data. In the two parameter space of the magnetic field (H) and the temperature (T), the FOPT can be attained by either varying H or T. H_cT_c is the value at which the local minima are equal in the free energy corresponding to competing phases and separated by a barrier. The disordered samples have a spatial distribution of H_cT_c values across the sample and the FOPT occurs in a certain range of H (or T). Thus, the H_cT_c line, representing the FOPT in the H–T plane, is broadened into a band for the disordered samples [13]. The high temperature phase persists below H_cT_c down to H^*T^*, below which even small fluctuations can transform the high temperature phase into a low temperature one. Similarly, the low temperature phase would persist above H_cT_c and up to $H^{**}T^{**}$, above which the small fluctuations can transform the low temperature phase into a high temperature one. The H^*T^* and $H^{**}T^{**}$ are named the supercooling and superheating limits, respectively, in this context. Like the H_cT_c line, the H^*T^* and $H^{**}T^{**}$ are also broadened into bands [13].

Figure 5 shows the H–T phase diagram, prepared from combining the results of the M–H, M–T and R–T measurements. The H_{up} (solid squares) and H_{dn} (open squares) values are determined as the magnetic field at which the first-order derivative of the M–H curve shows extrema in segment 1 and 2, respectively. The onset of the glassy state, as manifested by the splitting between ZFC and FCW observed in the M–T measurements under application of low fields,

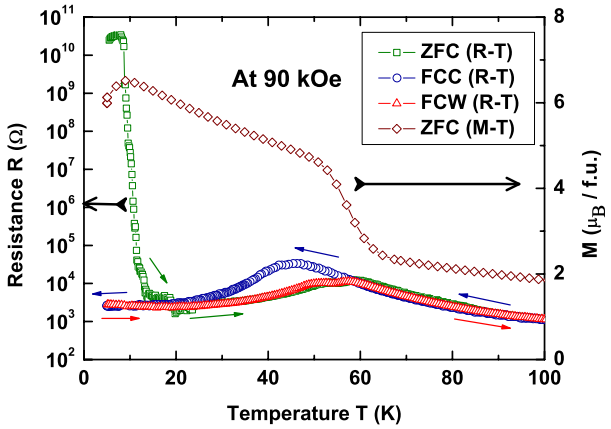

Figure 6. ZFC, FCC and FCW resistance measurements performed under application of a magnetic field of 90 kOe.

is represented by the points H_gT_g (tilted open triangles) in the phase diagram. The critical temperatures of transition from the FMM to COI phase for different magnetic fields are determined from the ZFC measurement as the extrema in the first derivative plot of M–T curve, and are denoted as open circles (M–$T_{(ZFC)}$). The critical temperatures, as determined by the minima in the second derivative plot of R–T curve, are denoted as open triangles (R–$T_{(ZFC)}$). Similarly, the critical temperatures of the reverse transition are determined from the FCC measurement and are denoted as solid circles (M–$T_{(FCC)}$) and solid triangles (R–$T_{(FCC)}$). The H_kT_k (solid star) values correspond to the transition from the insulating phase to the FMM phase observed at low temperature (see the discussion on figure 6) in zero field cooled R–T measurements. In this phase diagram, the superheating and supercooling limits are obtained from both the field and the temperature sweeping measurements.

Referring to figure 5, the critical field, H_{up}, decreases with a decrease in temperature down to ∼20 K. However, below 20 K, it starts increasing with a decrease in temperature. This non-monotonic behaviour is not reported in the earlier reports on GSMO. If at constant field, say H_1, the sample is cooled (horizontal line in the figure 5), then the supercooling limit is crossed at a certain temperature and a stable FMM phase is achieved by reaching a global free energy minimum. If the non-monotonic variation of H_{up} is considered to represent the supercooling limit, then further cooling will result in crossing the supercooling limit twice. The inflection point corresponding to the high temperature phase (COI) will once again develop in the free energy landscape. This is anomalous according to the classical concepts of FOPT [36]. The H_{up} represents the supercooling limit at higher temperatures above ∼20 K, while those calculated below this temperature would not be a true representation of the supercooling limit. Rawat *et al* [11], in their studies on NSMO, explained that the non-monotonic supercooling limit is anomalous. The present non-monotonic variation of H_{up} is similar to that reported in $La_{5/8-x}Pr_xCa_{3/8}MnO_3$ ($x = 0.41$) [13, 16].

In order to probe the observed anomaly in the H–T phase diagram of GSMO further, we have performed the R–T measurements under the application of constant magnetic fields: 85 and 90 kOe. The results obtained for 90 kOe are shown in figure 6. These measurements are performed by the four probe method using an SU. A very low magnitude of current ($\leqslant 10^{-7}$ A), corresponding to the linear part of the I–V characteristics, is used. The measurement protocol (ZFC, FCC and FCW) is similar to that employed in the M–T measurements, except that the measured physical quantity is resistance in this case. The temperature is swept at a ramp rate of ± 1 K min^{-1}. The ZFC resistance shows insulating behaviour at very low temperatures, followed by FMM phase. This is qualitatively consistent with the previous result on polycrystalline GSMO [37], where the ZFC resistance measurement was performed under 50 kOe.

In the ZFC measurements the sample is cooled from room temperature to 5 K, wherein T_{co} and T_g (glass transition) are progressively crossed and the sample is in the glassy insulator phase (referred to as the CG + COI phase in [29]). The field is then applied isothermally up to 90 kOe. According to the phase diagram (see figure 5), the field value has not yet crossed H_{up} and the sample is still insulating. The resistance is measured during the subsequent warming period to 100 K (see figure 6). Here, up to 9 K, the sample shows insulating behaviour, which is also reflected in the ZFC magnetization curve at the same field. Although the gross behaviour of this magnetization curve is similar to that in figure 3(b), where the sample was cooled to 3 K prior to the measurement, the low temperature behaviour is slightly different. Around 9 K, the resistance decreases sharply, which is an indication of the transition to the FMM phase. This is represented by the point H_kT_k (90 kOe, 9 K) in the H–T phase diagram. On further warming, the M–I transition is visible at around 59 K, which is also reflected as a decrease in the ZFC magnetization. The FCC measurement shows that a reverse (COI to FMM) transition takes place at a lower temperature (∼46 K). The thermal hysteresis is a manifestation of the FOPT. The sample remains in the metallic state down to 5 K, and its resistance is reversible until 15 K in the subsequent warming. Similar features are observed under an applied field of 85 kOe (figure not shown). In this case, the low temperature insulating phase transforms to the FMM phase at around 12 K. The FCC and FCW resistance curves are reversible below 19 K. Here, also, the ZFC and FCW resistance curves display noticeable splitting until they merge near 47 K. The most important feature observed in these isomagnetic R–T measurements is an open hysteresis loop in the first cycle: at very low temperatures the ZFC curve is found outside the FCW and FCC curves with marked differences in resistance magnitudes. This is an anomaly observed in a wide range of materials [10–14] for which kinetically arrested metastable states are considered to be responsible.

Referring to figure 5, the H_kT_k (or non-monotonic evolution of H_{up} at low temperatures) cannot be considered as the supercooling limit according to classical FOPT concepts. In the kinetic arrest model, this features as crossing the supercooling band causing hindrance to the FOPT. The temperature evolution of H_gT_g and H_kT_k suggests that there could be a connection between the two, which is likely to influence the FOPT in GSMO. This is schematically shown by the dotted band in the phase diagram.

4. Conclusions

In summary, single crystals of GSMO were grown by the float zone method. Detailed magnetotransport and DC magnetization measurements have been carried out across the FOPT between the COI and the FMM phases. Thermomagnetic anomalies, such as an open hysteresis loop in the M–H and the R–T measurements, are reported. The H–T phase diagram for GSMO is prepared using the M–H, M–T and R–T data. In the H–T plane, the temperature evolution of H_{up} is observed to be non-monotonic at temperatures below ∼20 K. Since the non-monotonic variation of the supercooling limit is anomalous, according to the classical ideas of FOPT, H_{up} values calculated below ∼20 K do not represent the supercooling limit. With this argument, even the H_kT_k is unsuitable to represent the supercooling limit. Accordingly, the open hysteresis loops in the R–T measurements cannot be explained solely on the basis of the supercooled metastable states. This calls for a thorough investigation of the observed thermomagnetic anomalies to confirm the nature of the metastable states (such as relaxation measurements) and to establish a possible link with the glassy behaviour in this system.

Acknowledgments

The authors acknowledge financial support from the DST, Government of India through the FIST programme. The National Facility for Low Temperature and High Magnetic Field is acknowledged for magnetotransport measurements. The authors, SE and HLB, thank DST for financial support through a project grant. The authors are grateful to A Banerjee for fruitful discussions and the UGC-DAE Consortium for Scientific Research, Indore for VSM measurements.

References

[1] Salamon M B and Jaime M 2001 *Rev. Mod. Phys.* **73** 583
[2] Tokura Y 2006 *Rep. Prog. Phys.* **69** 797
[3] Rodriguez-Martinez L M and Attfield J P 1996 *Phys. Rev.* B **54** R15622
[4] Hwang H Y, Cheong S-W, Radaelli P G, Marezio M and Batlogg B 1995 *Phys. Rev. Lett.* **75** 914
[5] Maignan A, Martin C, Van Tendeloo G, Hervieu M and Raveau B 1999 *Phys. Rev.* B **60** 15214
[6] Akahoshi D, Uchida M, Tomioka Y, Arima T, Matsui Y and Tokura Y 2003 *Phys. Rev. Lett.* **90** 177203
[7] Millange F, Caignaert V, Domenges B, Raveau B and Suard E 1998 *Chem. Mater.* **10** 1974
[8] Kuwahara H, Tomioka Y and Tokura Y 1995 *Science* **270** 961
[9] Tokura Y, Kuwahara H, Moritomo Y, Tomioka Y and Asamitsu A 1996 *Phys. Rev. Lett.* **76** 3184
[10] Manekar M A, Chaudhary S, Chattopadhyay M K, Singh K J, Roy S B and Chaddah P 2001 *Phys. Rev.* B **64** 104416
[11] Rawat R, Mukherjee K, Kumar K, Banerjee A and Chaddah P 2007 *J. Phys.: Condens. Matter* **19** 256211
[12] Banerjee A, Mukherjee K, Kumar K and Chaddah P 2006 *Phys. Rev.* B **74** 224445
[13] Kumar K, Pramanik A K, Banerjee A, Chaddah P, Roy S B, Park S, Zhang C L and Cheong S-W 2006 *Phys. Rev.* B **73** 184435
[14] Singh K J, Chaudhary S, Chattopadhyay M K, Manekar M A, Roy S B and Chaddah P 2002 *Phys. Rev.* B **65** 094419
[15] Ghivelder L and Parisi F 2005 *Phys. Rev.* B **71** 184425
[16] Sharma P A, Kim S B, Koo T Y, Guha S and Cheong S-W 2005 *Phys. Rev.* B **71** 224416
[17] Wu W, Israel C, Hur N, Park S, Cheong S W and Lozanne A D 2006 *Nat. Mater.* **5** 88
[18] Sharma P A, El-Khatib S, Mihut I, Betts J B, Migliori A, Kim S B, Guha S and Cheong S-W 2008 *Phys. Rev.* B **78** 134205
[19] Ward T Z *et al* 2009 *Phys. Rev. Lett.* **102** 087201
[20] Wu T and Mitchell J F 2006 *Phys. Rev.* B **74** 214423
[21] Smolenskii G A and Chupis I E 1982 *Usp. Fiz. Nauk* **137** 415
[22] Huang Z J, Cao Y, Sun Y Y, Xue Y Y and Chu C W 1997 *Phys. Rev.* B **56** 2623
[23] Wang J *et al* 2003 *Science* **299** 1719
[24] Kimura T, Kawamoto S, Yamada I, Azuma M, Takano M and Tokura Y 2003 *Phys. Rev.* B **67** 180401(R)
[25] Fiebig M, Lottermoser Th, Frohlich D, Goltsev A V and Pisarev R V 2001 *Nature* **419** 818
[26] Kimura T, Goto T, Shintani H, Ishizaka K, Arima T and Tokura Y 2003 *Nature* **426** 55
[27] Kimura T, Lawes G, Goto T, Tokura Y and Ramirez A P 2005 *Phys. Rev.* B **71** 224425
[28] Kadomtseva A M, Popov Yu F, Vorob'ev G P, Ivanov V Yu, Mukhin A A and Balbashov A M 2005 *JETP Lett.* **82** 590
[29] Garcia-Landa B, De Terasa J M and Ibarra M R 1998 *J. Appl. Phys.* **83** 7664
[30] Shannon R D 1976 *Acta Crystallogr.* A **32** 751
[31] Kostogloudis G C H and Ftikos C H 1999 *J. Mater. Sci.* **34** 2169
[32] Woodward P M 1998 *Chem. Mater.* **10** 3652
[33] Terai T, Sasaki T, Kakeshita T, Fukuda T, Saburi T, Kitagawa H, Kindo K and Honda M 2000 *Phys. Rev.* B **61** 3488
[34] Sun Y, Salamon M B, Tong W and Zhang Y 2002 *Phys. Rev.* B **66** 094414
[35] Snyder G J, Booth C H, Bridges F, Hiskes R, Dicarolis S, Beasley M R and Geballe T H 1997 *Phys. Rev.* B **55** 6453
[36] Chaikin P M and Lubensky T C 1995 *Principles of Condensed Matter Physics* (Cambridge: Cambridge University Press)
[37] Damay F, Maignan A, Martin C and Raveau B 1997 *J. Appl. Phys.* **81** 1372